Journal of Hazardous Materials 193 (2011) 17–26

Contents lists available at ScienceDirect

Journal of Hazardous Materials

journal homepage: www.elsevier.com/locate/jhazmat

Development of adsorbent from Teflon waste by radiation induced grafting: Equilibrium and kinetic adsorption of dyes

N.K. Goel, Virendra Kumar, S. Pahan [1], Y.K. Bhardwaj*, S. Sabharwal

Radiation Technology Development Division, Bhabha Atomic Research Centre, Trombay, Mumbai 400 085, India

ARTICLE INFO

Article history:
Received 17 January 2011
Received in revised form 27 April 2011
Accepted 9 May 2011
Available online 14 May 2011

Keywords:
Radiation
Grafting
Teflon scrap
Acrylic acid
Adsorption
Basic dyes

ABSTRACT

Mutual radiation grafting technique was employed to graft polyacrylic acid (PAA) onto Polytetrafluoroethylene (Teflon) scrap using high energy gamma radiation. Polyacrylic acid-*g*-Teflon (PAA-*g*-Teflon) adsorbent was characterized by grafting extent measurement, FTIR spectroscopy, SEM and wet ability & surface energy analysis. The PAA-*g*-Teflon adsorbent was studied for dye adsorption from aqueous solution of basic dyes, namely, Basic red 29 (BR29) and Basic yellow 11 (BY11). The equilibrium adsorption data were analyzed by Langmuir and Freundlich adsorption isotherm models, whereas, adsorption kinetics was analyzed using pseudo-first order, pseudo-second order and intra-particle diffusion kinetic models. Equilibrium adsorption of BR29 was better explained by Langmuir adsorption model, while that of BY11 by Freundlich adsorption model. The adsorption capacity for BY11 was more than for BR29. Separation factor (R_L) was found to be in the range $0 < R_L < 1$, indicating favorable adsorption of dyes. Higher coefficient of determination ($r^2 > 0.99$) and better agreement between the $q_{e,cal}$ and $q_{e,exp}$ values suggested that pseudo-second order kinetic model better represents the kinetic adsorption data. The non-linearity obtained for intra-particle diffusion plot indicated, more than one process is involved in the adsorption of basic dyes. The desorption studies showed that ~95% of the adsorbed dye could be eluted in suitable eluent.

1. Introduction

Synthetic dyes represent a relatively large group of organic chemicals, encountered practically in all spheres of daily life. Various kinds of synthetic dyestuffs appear in the effluents of industries, such as textile, leather, paper printing and plastic industry [1,2]. Release of these dyes in water stream is not only aesthetically undesirable but also has a serious environmental impact. Due to intense color they reduce sunlight transmission into water hence affecting photosynthesis phenomenon causing adverse effect on the growth of bacteria and fungi, aquatic plants and other form of aquatic life, which ultimately disturb aquatic ecosystem and food chain [3]. Increased public concern, ecological awareness, as well as strict regulation enforcement by concerned authorities regarding effluent quality have forced industry to pre-treat effluents before discharging and to look for other economically viable ways to treat the effluents. It is now established that only few dyes can be microbiologically degraded under anaerobic condition, which in most cases leads to the generation of carcinogenic compounds [4,5] and mutagens [6]. Majority of the textile dyes because of their complex aromatic structure are difficult to mineralize. Moreover, due to industry demand dye producers are being forced to produce dyes of higher stability and fastness, which are more difficult to degrade [2,7]. World wide efforts are on to mitigate the possible harm to the environment due to release of dyes to aqueous streams either by removing the dyes or by degrading them to harmless products. Physico-chemical methods, such as adsorption, coagulation, precipitation, filtration, oxidation by ozone treatment, chemical oxidation, photo-catalytic processes, biological treatment and ionizing radiation degradation have been proposed for dye effluent treatment [8]. However most of the proposed processes are either economically unviable or are inadequate to treat high concentration of large volume of industrial effluents. The adsorption process has been found to be comparatively simple, effective and efficient technique for dye removal from waste-water. Many adsorbents such as activated carbon, peat, chitin, coir pith, banana and orange peel, silica, etc. have been tried for the purpose. The adsorbents like activated carbon have high cost while adsorbents of natural origin suffer from the low adsorption capacity. The need is for cost-effective, recyclable adsorbent system, which can treat typical high concentration of hundreds of ppm of dyes usually found in industrial waste-water effluents [9].

Polytetraflouroethylene (PTFE), commercially known as 'Teflon', has been used for numerous applications because of its exceptional

* Corresponding author. Fax: +91 022 25505151.
E-mail address: ykbhard@barc.gov.in (Y.K. Bhardwaj).
[1] Present address: Process Development Division, Bhabha Atomic Research Centre, Trombay, Mumbai 400 085, India.

0304-3894/$ – see front matter © 2011 Published by Elsevier B.V.
doi:10.1016/j.jhazmat.2011.05.026

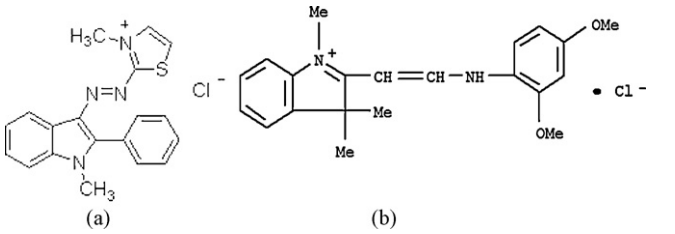

Fig. 1. Structure of basic dyes used for studies (a) Basic Red 29 (λ_{max} = 508 nm) (b) Basic Yellow 11 (λ_{max} = 411 nm).

properties like, hydrophobic, inert, excellent chemical resistant, non-stick characteristics, outstanding performance at extreme temperatures, low coefficient of friction, etc. [10,11]. However, the exceptional properties of Teflon pose the hindrance for its scrap disposal, as it does not undergo degradation under natural conditions. The objective of the present work is to develop good capacity anionic adsorbent from Teflon scrap using radiation technology for waste-water treatment applications. Radiation induced grafting technique has been proved to be an easy and highly efficient technique for incorporating desired chemical groups onto existing polymer substrates without altering the bulk properties of base polymer [12,13]. Radiation grafting leads to desired functional polymer brushes, which have got applications in separation and immobilization of biomolecules [14]. In present work, mutual radiation grafting technique is employed to convert Teflon scrap into a valuable adsorbent by radiation induced grafting of polyacrylic acid onto the Teflon to obtain Teflon matrix having covalently linked anionic groups (–COOH) using ^{60}Co gamma radiation source. The radiation grafted PAA-*g*-Teflon adsorbent was investigated for removal of basic dyes BR29 and BY11 from manufactured aqueous dye solutions followed by desorption of adsorbed dye using suitable eluents.

The widely used Langmuir [15] and Freundlich [16], isotherm models, were employed to analyze the equilibrium adsorption of basic dyes onto PAA-g-Teflon. The adsorption kinetic data was analyzed using pseudo-first-order [17], pseudo-second-order [18] and desorption diffusion model equation [19].

2. Experimental

2.1. Materials

Teflon scrap in ribbon form, obtained after machining of Teflon rods, was procured from local supplier M/s Max Tools Co. Mumbai, India. The Teflon samples were washed with toluene followed by detergent solution and finally vacuum dried at 50 °C and stored in desiccator for further use in radiation grafting process. The cleaned Teflon scrap has a bulk density = 2.1 g/cc, Melting point = 330 °C and surface energy = 22.5 mJ/m^2. Acrylic acid monomer (purity >97%) from M/s Prabhat Chemicals, Mumbai was used as received. Mohr's salt and sulfuric acid were of AnalaR (Purity >99%) grade. Double distilled water was used for preparation of all the solutions. The basic dyes, namely Basic Red 29 (BR29, dye content ca. 20%), Basic yellow 11 (BY11, dye content ca. 20%) were procured from Sigma–Aldrich. The chemical structures of dyes are given in Fig. 1.

2.2. Radiation source

Gamma chamber (GC 5000, BRIT, INDIA) having ^{60}Co gamma radiation source, supplied by M/s BRIT, India having dose rate of 2.5 kGy h^{-1} as determined by Fricke dosimetry was used for irradiation purpose for radiation induced grafting of AA on to Teflon substrate.

2.3. Radiation grafting

Mutual radiation grafting technique was used to graft acrylic acid (AA) onto Teflon substrates under the parameters standardized as reported in earlier part of this study [20]. A known amount of Teflon samples were immersed in to the aqueous grafting solution, containing 20 wt.% AA, 4 wt.% Mohr's salt and 0.5 mol dm^{-3} of H_2SO_4 in the stoppered glass bottles for an hour. The glass bottles were then irradiated in gamma chamber for desired doses at dose rate of 2.5 kGy h^{-1}. The grafted samples were washed with double distilled water in a soxhlet extraction assembly for 8 h in order to remove poly(acrylic acid) homopolymer trapped in the grafted Teflon. Finally the grafted samples were dried under vacuum at 50 °C and stored for further studies.

2.4. Grafting yield determination

After radiation grafting of acrylic acid on to the Teflon substrates the PAA-g-Teflon samples were characterized by grafting yield (G.Y.) determined gravimetrically using relation (1)

$$\text{Grafting yield (\%)} = \left[\frac{\text{Weight after grafting} - \text{Initial weight}}{\text{Initial weight}}\right] \times 100 \quad (1)$$

2.5. FTIR analysis

The grafting of AA onto Teflon was confirmed by Fourier transformed infra red (FTIR) spectroscopy using FTIR spectrophotometer (JASCO, FT/IR-610) in ATR mode. The samples were pressed inside the sample holders and the spectra recorded in the range 400–4000 cm^{-1} with a resolution of 4 cm^{-1} and averaged over 100 scans.

2.6. Scanning electron microscopy (SEM)

The morphology of the pristine and PAA-g-Teflon was investigated by Scanning Electron Microscopy (SEM) analysis using VEGA MV2300T/40 (TS 5130 MM) microscope (TESCAN) at acceleration voltages of 30 kV. The bulk morphology of the samples was analyzed by taking cross-sectional images of fractured samples after coating with thin layer of gold under vacuum and pasted on a conducting surface by carbon paste.

2.7. Wet ability and surface energy analysis

The modified surface of Teflon (due to radiation grafting) was characterized by its water contact angle (WCA) measurements. The contact angle measurement of the sample was carried out by sessile drop technique using image analysis software. A liquid droplet (1.5–2.5 μL) was allowed to fall on the samples to be studied from a software-controlled syringe. An image sequence was taken through a CCD camera of goniometer from GBX instruments, France which was connected to a computer and interfaced to image capture software (Windrop^{++}, GBX instruments).

Surface energy of samples was estimated by static contact angle values measured for two probe liquids, namely water and diiodomethane using Owens and Wendent geometric mean Eq. (2) [21]

$$(1 + \cos\theta)\,\gamma_l = 2[(\gamma_s^d \gamma_l^d)^{1/2} + (\gamma_s^p \gamma_l^p)^{1/2}] \quad (2)$$

and

$$\gamma_s = \gamma_s^p + \gamma_s^d \quad (3)$$

where θ is the contact angle, γ_s and γ_l are the surface free energies of the solid and liquid, respectively. The superscripts 'd' and 'p' refer to the dispersive and polar components of surface energy, respectively.

2.8. Adsorption of dyes

For equilibrium adsorption experiments, stock solutions of basic dyes BR29 and BY11 of concentration of 1000 mg/L were prepared in double distilled water and later diluted as required for equilibrium and kinetic adsorption study. A known mass (0.05 g) of PAA-*g*-Teflon adsorbent (G.Y. ~30%) was weighed into 100 mL stoppered conical flasks and allowed to equilibrate with 50 mL of aqueous dye solution of known concentration. Dye concentrations in the solutions were estimated spectrophotometerically using UV/Vis spectrophotometer (Evolution-300, Thermoelectron Corporation, Ltd., UK) using calibration curves established for each dye, at wavelength corresponding to the maximum absorbance, i.e., λ_{max} = 411 nm and 508 nm for BY11 and BR29, respectively. The equilibrium adsorption amounts of dye onto adsorbent q_e (mg/g) were estimated by using Eq. (4)

$$q_e = \frac{(C_i - C_e)V}{m.1000} \quad (4)$$

where C_i and C_e are the initial and equilibrium concentrations (mg/L) of dye, respectively; and V (mL) is the volume of the dye solution and m (g) is the mass of the adsorbent.

For kinetic studies, 0.1 g of PAA-g-Teflon adsorbent (G.Y. ~30%) was taken in 100 mL of dye solutions of concentration 400 mg/L at pH ~4.7, maintained using phosphate buffer at 28 °C. The adsorption kinetics of dyes was followed by monitoring the dye concentration, remaining in the aqueous solution spectrophotometerically at different time intervals.

2.9. Desorption studies

Desorption experiments were carried out by immersing the PAA-g-Teflon adsorbent-loaded with basic dyes, in 40 mL of desorption solution containing 1N KSCN in varying water–methanol mixture, for 12 h at room temperature. The desorbed dye concentration was estimated spectrophotometerically after suitable dilution. The quantity of desorbed dye was quantified in terms of desorption percentage, estimated using relation (5)

$$\%\,\text{De-sorption} = \left(\frac{W_{Des}}{W_{Ad}}\right) \times 100 \quad (5)$$

where W_{Ad} and W_{Des} are the amount of adsorbed and desorbed dye.

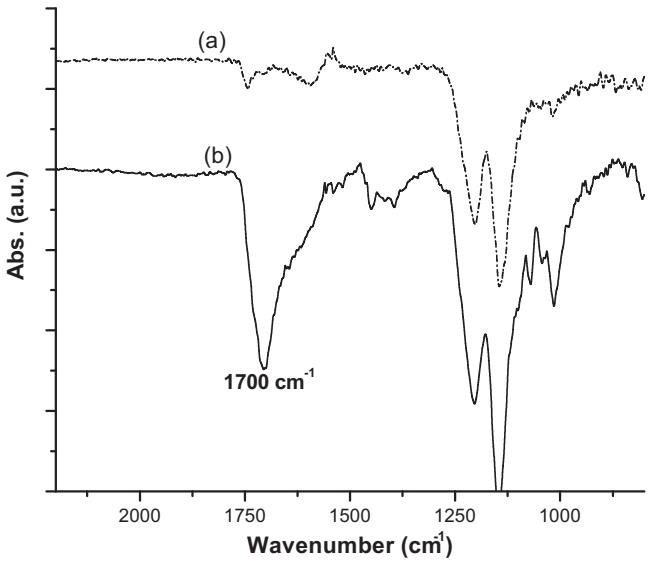

Fig. 2. FTIR spectra of (a) Pristine Teflon (b) PAA-g-Teflon samples (G.Y. ~8.5%).

3. Results and discussion

3.1. FTIR analysis of grafted samples

The FTIR spectra of pristine Teflon and PAA-g-Teflon samples (grafting extent ~30%) are shown in Fig. 2. For pristine PTFE, the expected absorbance peaks at 1145 cm^{-1} and 1205 cm^{-1} due to CF_2 symmetric and asymmetric stretching, respectively, were observed. Grafting of PAA on to Teflon was confirmed by appearance of the additional peaks in PAA-g-Teflon, namely, a strong absorbance peak at ~1700 cm^{-1} due to the stretching vibration of >C=O, and peaks at 1450 and 1395 cm^{-1} attributed to the CH_2 deformation bands from the PAA grafted chains.

3.2. Scanning electron microscopy (SEM)

Fig. 3 shows the SEM images of pristine Teflon and PAA-g-Teflon, which clearly revealed the difference in the bulk morphology of pristine Teflon and PAA-g-Teflon samples. The grafting of PAA on to Teflon substrate clearly results in reduction in compactness of pristine Teflon structure due to formation of pores and voids.

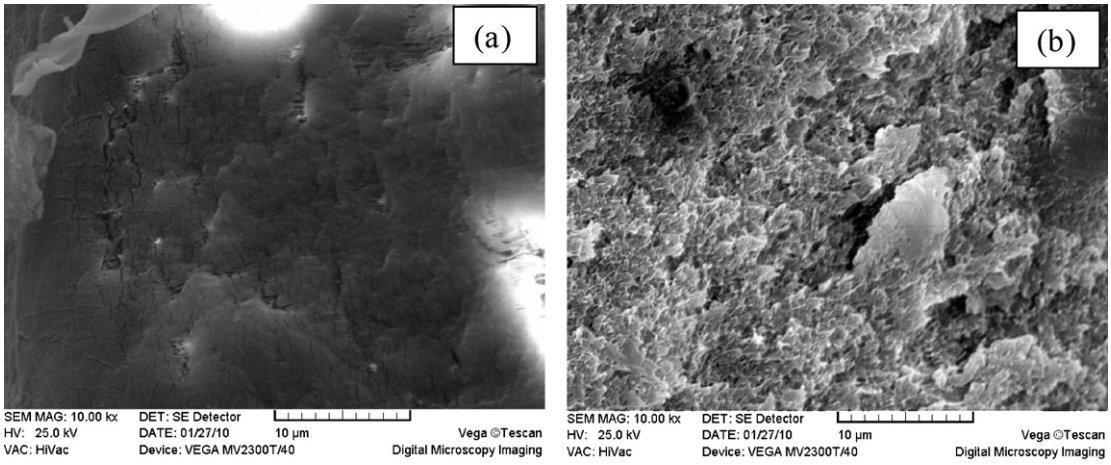

Fig. 3. SEM micro-images presenting bulk morphology of (a) Pristine Teflon (b) PAA-g-Teflon (G.Y. ~30%).

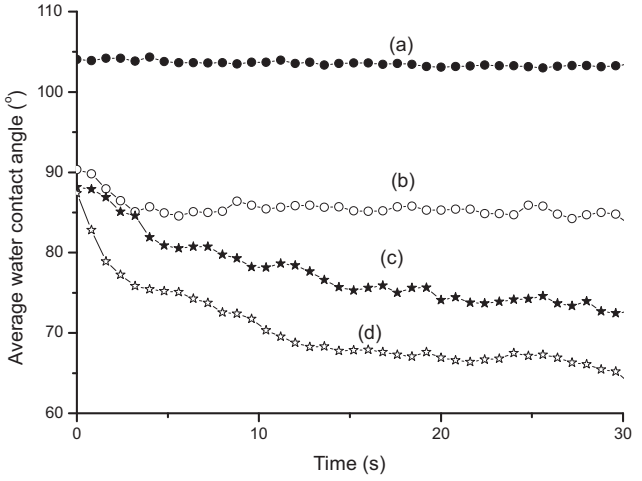

Fig. 4. Contact angle of samples with water (a) PTFE (b) PTFE grafted to an extent of 8.5% (c) PTFE grafted to an extent of 16.0% (d) PTFE grafted to an extent of 23.5%.

3.3. Wet ability and surface energy analysis

Fig. 4 shows the contact angle of water with pristine Teflon and PAA-g-Teflon sample with varying G.Y., recorded in kinetics mode. It can be seen that the water contact angle of Teflon was ~105°, indicating its hydrophobic nature (WCA > 90°), and the contact angle of Teflon does not change with time. The grafting of AA results in decrease in water contact angle of Teflon (WCA < 90°), indicating hydrophilic character of PAA-g-Teflon [22]. The WCA of PAA-g-Teflon decreases with the increase in grafting yield. In addition, the WCA of PAA-g-Teflon gradually decreases with time, which is attributed to the polar interaction of water with –COOH group of grafted PAA chains. The total surface energy and the values of its resolved components, i.e., polar and dispersive, of different samples with varying G.Y., are given in Table 1. The total surface energy of Teflon indicates its inert nature. There was a significant increase in total surface energy of PAA-g-Teflon samples with increase in grafting yield, which was mainly due to increase in the polar energy component of PAA. The higher surface energy and hydrophilic character of PAA-g-Teflon would facilitate the adsorption of cationic dyes onto it.

3.4. Effect of absorbed dose on grafting yield

The number of grafted chains in mutual radiation process is a function of total absorbed dose, as it governs the total number of free radicals generated on the trunk polymer [23]. The effect of absorbed dose was studied by carrying out the grafting reaction at different gamma absorbed doses. Inset Fig. 5 shows result of this study. Under optimized experimental conditions, the G.Y. increased almost linearly with absorbed dose in the dose range 0–13 kGy in accordance with Eq. (6). The increase in absorbed dose proportionally increases the number of radical grafting sites on the trunk polymer leading to more number of grafting chains initiated resulting into higher grafting yield.

$$\text{G.Y.}(\%) = 1.47 + 5.62 \times \text{Dose}\,(\text{kGy}) \quad (6)$$

Table 1
Surface energy of samples.

Grafting extent	Surface energy (mJ/m^2)		
	Total energy	Polar component	Dispersive component
Nil	22.5	1.2	21.3
8.5%	29.1	4.3	24.8
16.0%	34.3	9.7	24.6
23.5%	43.4	17.8	25.6

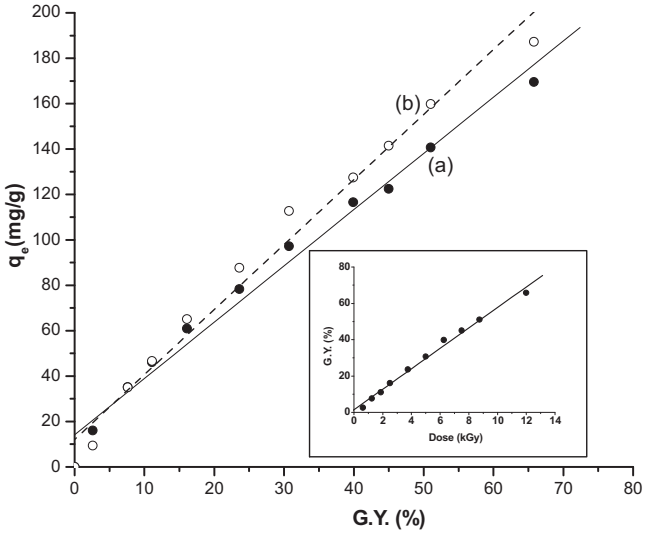

Fig. 5. Adsorption of dyes on to PAA-g-Teflon grafted to different extents; [Dye] = 400 mg/L. (a) BR29, (b) BY11. Inset: Effect of absorbed dose on grafting yield at dose rate of 2.5 kGy h^{-1}.

3.5. Effect of grafting yield on dye adsorption

Fig. 5 shows the relation of the dye adsorption capacity of PAA-g-Teflon with G.Y., which reveals a linear increase in the adsorption capacity of the PAA-g-Teflon adsorbent with the increase in the G.Y. The results are on the expected lines as the increase in the grafting yield would increase the concentration of the primary adsorption sites, i.e., COOH groups, which will attract more numbers of oppositely charged dye molecules, manifested by increased adsorption capacity of the radiation grafted adsorbent [20]. In addition, the increase in the grafting yield was found to increase the surface energy, i.e., wettability or hydrophilicity of the PAA-g-Teflon (Fig. 4), which facilitates the approach of dye molecules towards the PAA-g-Teflon adsorbent.

3.6. Equilibrium adsorption of dyes

Dye adsorption is a process governed by mass transfer, which can be understood by equilibrium isotherms and kinetic models. An equilibrium is established when the amount of solute being adsorbed onto the adsorbent is equal to the amount being desorbed. Adsorption isotherms describe how adsorbates interact with adsorbents and so are critical in optimizing the use of adsorbents. Therefore, rigorous treatment of equilibrium adsorption data using theoretical or empirical equations is essential for practical application of the adsorbent. In present study, two widely used equilibrium isotherm models, namely, Langmuir [15] and Freundlich isotherm models [16] were used to analyze the experimental adsorption data, using coefficient of determination (r^2) as criteria for selecting best fit isotherm model [24]. Figs. 6 and 7 represent the equilibrium adsorption isotherm plots of PAA-g-Teflon for BR29 and BY11 dyes at different solution temperatures.

3.6.1. Langmuir adsorption isotherms

Langmuir adsorption model initially proposed for adsorption of gases onto metal surfaces later found successful application in

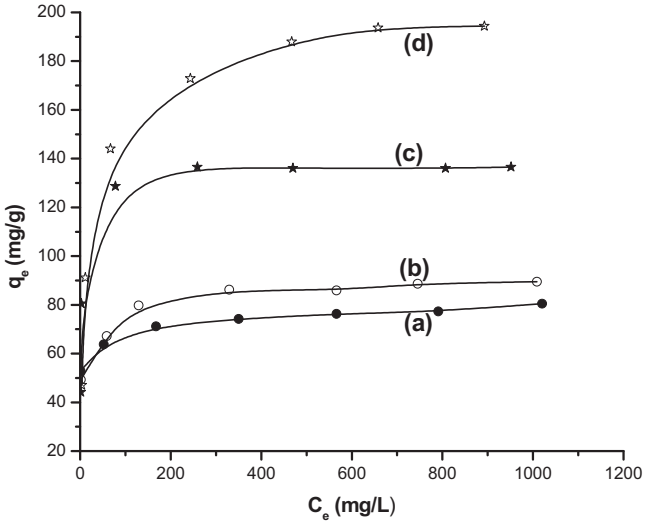

Fig. 6. Equilibrium adsorption isotherms of grafted matrices (G.Y. ~30%) for basic dye BR29 at different temperatures (a) 28 °C (b) 40 °C (c) 50 °C (d) 60 °C.

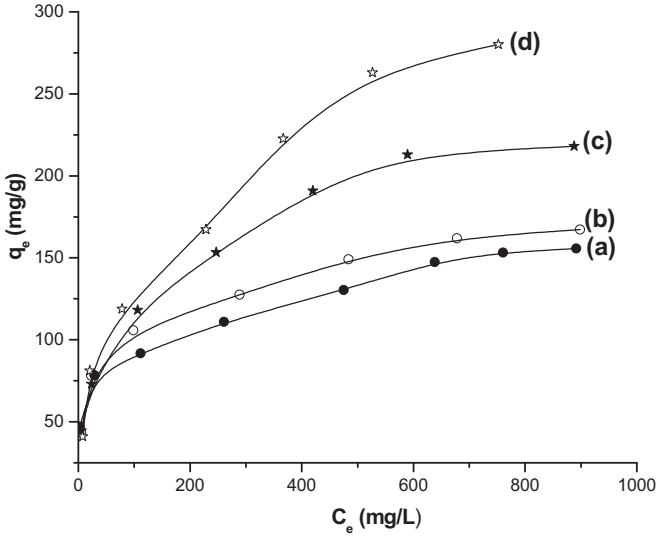

Fig. 7. Equilibrium adsorption isotherms of grafted matrices (G.Y. ~30%) for basic dye BY11 at different temperatures (a) 28 °C (b) 40 °C (c) 50 °C (d) 60 °C.

many other real sorption processes involving monolayer adsorption [12,15,25]. Langmuir's model based on certain assumptions [15] postulates that theoretically adsorbent has a finite capacity for the adsorbate; therefore saturation is reached beyond which no

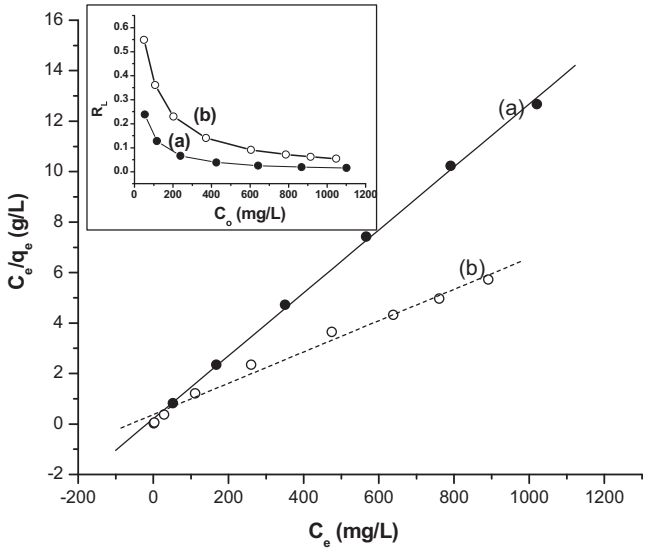

Fig. 8. Langmuir adsorption isotherms for dye adsorption on PAA-g-Teflon (G.Y. ~30%) at 28 °C (a) BR29 (b) BY11. Inset: Separation factor (R_L) for adsorption of dyes at 28 °C, as a function of initial concentration (C_o) of dyes (a) BR29, (b) BY11.

further adsorption takes place. Langmuir isotherm model is represented by expression (7)

$$q_e = \frac{K_L C_e}{1 + a_L C_e} \tag{7}$$

where q_e is the solid-phase dye concentration at equilibrium (mg/g), C_e is the liquid-phase dye concentration at equilibrium (mg/L); K_L (L/g) and a_L (L/mg) are the Langmuir isotherm constants. Generally used and more easier and convenient form of Langmuir equation is its linear form (Eq. (8))

$$\frac{C_e}{q_e} = \frac{1}{K_L} + \frac{a_L}{K_L} C_e \tag{8}$$

Linear plots of C_e/q_e *vs* C_e give straight lines with slope a_L/K_L and intercept $1/K_L$. The theoretical monolayer saturation capacity q_{max} (mg/g) can be evaluated from the langmuir equilibrium constants K_L (L/g) and a_L (L/mg) using Eq. (9)

$$q_{max} = \frac{K_L}{a_L} \tag{9}$$

Fig. 8 shows linear Langmuir isotherms for adsorption of the two dyes. Langmuir adsorption parameters obtained from these isotherm plots are presented in Table 2. The linearity of isotherms and high coefficient of determination values (r^2 ~0.999) and degree of agreement between q_{exp} and q_{max} values predicted from Langmuir isotherm model for adsorption of dye BR29 suggested that BR29 adsorption follows the Langmuir model over the whole concentration range studied. On the other hand, for BY11 the comparatively lower r^2 values and poor agreement between q_{exp} and

Table 2
Langmuir and Freundlich adsorption parameters for adsorption of dyes by PAA-g-Teflon adsorbent.

	Langmuir						Freundlich		
	Temp. (°C)	$q_{e,exp}$ (mg/g)	K_L (L/g)	Dyes	q_{max} (mg/g)	r^2	K_F (L/g)	n	r^2
BR29	28	80.5	4.76	0.059	80.2	0.9987	51.6	16.26	0.9874
BY11	28	156.0	2.65	0.016	161.3	0.9861	37.5	4.85	0.9867
BR29	40	89.5	6.28	0.070	89.6	0.9992	46.8	10.22	0.9729
BY11	40	167.2	3.49	0.020	171.2	0.9822	31.7	3.99	0.9804
BR29	50	136.6	53.4	0.390	136.8	0.9999	55.8	6.86	0.8137
BY11	50	218.1	3.19	0.014	232.5	0.9881	26.0	3.09	0.9962
BR29	60	194.3	9.34	0.047	198.4	0.9994	42.5	4.12	0.9117
BY11	60	280.1	3.02	0.009	305.8	0.9688	20.4	2.49	0.9832

q_{max} values predicted from Langmuir model suggested that Langmuir model does not fit well to the adsorption of BY11, particularly at higher temperatures. The adsorption capacity of PAA-g-Teflon for BY11 was found to be higher than that for BR29, which could be attributed to their different molecular structures. The higher adsorption capacity for BY11 may be due to higher polarity and hydrophilicity of BY11 dye due to presence of methoxy group in its molecular structure.

The Langmuir adsorption constant a_L (L/mg), can be used to determine a dimensionless separation factor R_L [26], defined by Eq. (10)

$$R_L = \frac{1}{(1 + a_L C_o)} \tag{10}$$

where C_o is the initial dye concentration (mg/L). The value of parameter R_L indicates the nature of the adsorption process [26]. (i) $R_L > 1$ for unfavorable adsorption, (ii) $R_L = 1$ for linear adsorption, (iii) $0 < R_L < 1$ for favorable adsorption, and (iv) $R_L = 0$ for irreversible adsorption. The variation in R_L with initial dye concentration is shown in Inset Fig. 8. As shown in figure R_L value decreased with the increase in C_o. In concentration range 50–1100 mg/L, the R_L values were in range $0.24 < R_L < 0.02$ and $0.55 < R_L < 0.05$ for BR29 and BY11, respectively. R_L values for adsorption of both dyes lie in between 0 and 1 indicating reversible and favorable adsorption of dyes onto PAA-g-Teflon adsorbent. It was clear from R_L values that with the increase in the initial dye concentration, the adsorption of basic dyes shifted from favorable adsorption towards irreversible adsorption.

3.6.2. Freundlich adsorption isotherm

Freundlich isotherm is an empirical equation employed to describe heterogeneous systems, expressed as follows [16]

$$q_e = K_F C_e^{1/n} \tag{11}$$

$$\text{or } \ln(q_e) = \ln(K_F) + (1/n)\ln(C_e) \tag{12}$$

where q_e is the solid-phase dye concentration at equilibrium (mg/g), C_e is the liquid-phase dye concentration at equilibrium (mg/L), K_F is the Freundlich constant (L/mg), and $1/n$ is the heterogeneity factor. The Freundlich isotherm is derived assuming an exponential decay energy distribution function inserted into the Langmuir equation. Unlike Langmuir model it describes reversible adsorption and is not restricted to the formation of the monolayer. The amount of adsorbed material is the summation of adsorption on all binding sites. The Freundlich equation predicts that the dye concentrations on the adsorbent will increase as long as there is an increase in the dye concentration in the solution. An exponent (n) value between 1 and 10 represents beneficial or favorable adsorption [26]; higher the n value, the stronger the adsorption intensity. K_F has been used as indicative parameter of the adsorption strength; higher value of K_F indicates a higher capacity of adsorption [24].

The equilibrium adsorption data for BR29 and BY11 was plotted in the linear form of Freundlich isotherm (Eq. (12)) from which the Freundlich constants K_F and Freundlich exponent n were determined from the intercept and the slope of the plot, respectively (Fig. 9). The values for Freundlich isotherm parameters are shown in Table 2. At 28 °C, the correlation coefficients for Freundlich model were >0.98 for both the dyes. The $n > 1$ values with high K_F values indicated beneficial and favorable adsorption of BR29 and BY11 with high adsorption capacity of PAA-g-Teflon adsorbent.

3.6.3. Effect of temperature on adsorption of dyes on PAA-g-Teflon

The equilibrium adsorption experiments were carried out at varying solution temperature to investigate the effect of the temperature on the adsorption isotherm parameters (Table 2). The

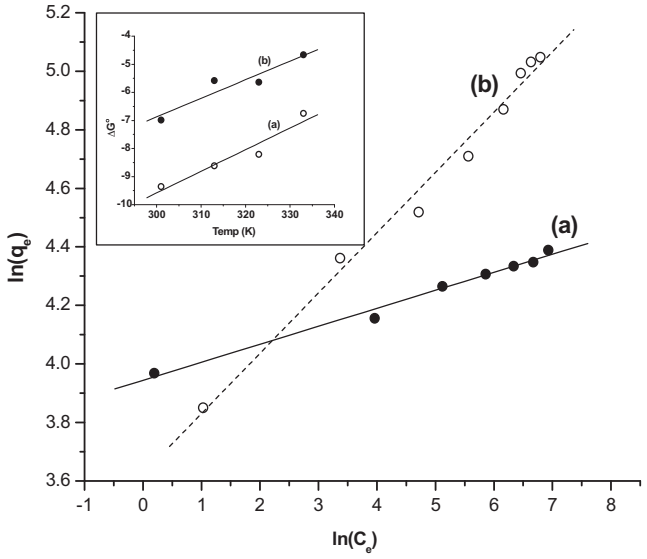

Fig. 9. Linear Freundlich adsorption plots for adsorption of dyes on PAA-g-Teflon (G.Y. ~30%) at 28 °C (a) BR29 (b) BY11. Inset: Effect of temperature of standard free energy change for adsorption [Dye] = 50 mg/L (a) BR29 (b) BY11.

adsorption capacity of PAA-g-Teflon increased with the increase in the solution temperature. This can be explained on the basis of opening up of entangled grafted PAA chains increasing their flexibility and thus providing more sites for dye adsorption at higher temperature. Moreover, the increase in temperature would facilitate the mobility of dye molecules and allow diffusion of the large dye molecules across the external boundary layer and into internal pores of the adsorbent. For both the dyes, the values of Freundlich exponent 'n' decreased with the increase in the temperature, indicating decrease in adsorption intensity at higher temperature. Comparing the values obtained from two models for the dyes (Table 2), it was observed that for BR29, the r^2 for Freundlich model decreased at higher temperatures, whereas, r^2 for Langmuir model remained constant. In addition, for BR29, the q_{max} values predicted by Langmuir model were in good agreement with the $q_{e,exp}$ values at all the temperatures. On the contrary, for BY11, the r^2 for Freundlich model were not affected by temperature; and there was a significant difference between the q_{max} and $q_{e,exp}$ values and difference increased with temperature. These observations indicated that in the temperature range studied, Langmuir adsorption isotherm model better describes the equilibrium adsorption of BR29, whereas, Freundlich adsorption isotherm model better explains the adsorption of BY11.

3.6.4. Estimation of the thermodynamic parameters

An investigation on temperature dependence of dye adsorption was used to obtain valuable information on thermodynamic adsorption parameters, such as change in standard Gibbs free energy (ΔG°), enthalpy (ΔH°) and entropy (ΔS°). The Gibbs free energy change (ΔG°) of the adsorption process is related to the equilibrium constant by Eq. (13) [27,28]

$$\Delta G^\circ = -RT \ln K_c \tag{13}$$

where T is the temperature of solution (K), R is the universal gas constant (8.314 J/mol K) and K_c is the distribution coefficient for adsorption, which was estimated using Eq. (14) [27,28]

$$K_c = \frac{C_{Ae}}{C_e} \tag{14}$$

where C_{Ae} the amount of dye (mg) adsorbed on the adsorbent per liter of the solution at equilibrium, and C_e is the equilibrium concen-

Table 3
Thermodynamic parameters for the adsorption of dyes on PAA-g-Teflon.

Dye	Temp. (K)	ΔG^o (kJ/mol)	ΔH^o (kJ/mol)	ΔS^o(kJ/mol)
BY11	301	−6.989		
	313	−5.582	−26.709	−0.066
	323	−5.636		
	333	−4.659		
BR29	301	−9.359		
	313	−8.613	−32.686	−0.702
	323	−8.212		
	333	−6.752		

tration (mg/L) of dye in the solution. The Gibbs free energy change (ΔG°) is related to ΔH° and ΔS° by Eq. (15) [25,27]

$$\Delta G^\circ = \Delta H^\circ - T\Delta S^\circ \quad (15)$$

The values of ΔH° and entropy (ΔS°) for adsorption were estimated from slope and intercept of the linear plot of ΔG° *vs* T (Inset Fig. 9).

The values of adsorption thermodynamic parameters are listed in Table 3. The negative value of ΔG° confirms the feasibility of the adsorption process and also indicates spontaneous adsorption of basic dyes on PAA-g-Teflon adsorbent in the temperature range studied, which is usually the case for many adsorption systems consisting of oppositely charged adsorbate–adsorbent systems. The negative ΔH° value indicates the adsorption process to be exothermic due to formation of ionic bond between the cationic dye and the anionic carboxylic group of the PAA-g-Teflon. The negative ΔS° value indicates the decrease in disorderness on adsorption. Similar negative values for ΔH° and ΔS° for adsorption of reactive dyes on other polymeric systems have been reported [17]. However, our observation reported in Section 3.3 about the increase in adsorption capacity of PAA-g-Teflon with the increase in the temperature is in contradiction to the thermodynamic results, i.e., negative value of ΔH°. This can be explained on the basis of influence of medium temperature on two competitive opposite effects. The increase in temperature would (i) The decrease dye adsorption due to the dissociation of ionic bonds, and (ii) Increase adsorption due to increase in the mobility and diffusion of dye molecules through the open up structure of the adsorbent. The results suggested that the later effect dominates over the former one, resulting in the increased dye adsorption at higher temperatures.

3.7. Adsorption kinetics

The second vital evaluation element for an adsorption operation unit is the adsorption kinetics, i.e., rate of adsorption reaction, which depends on the adsorbate–adsorbent interaction and system condition. Adsorbate uptake rate determines the residence time required for completing the adsorption reaction and can be enumerated from kinetic analysis using different kinetic models. Numerous attempts were made in formulating a general expression to describe the kinetics of adsorption on solid surfaces for the liquid–solid adsorption system. In the present work, pseudo-first-order [17] and pseudo-second-order kinetic models [18] were used to determine the rate of adsorption of dyes onto PAA-g-Teflon adsorbent. The adsorption kinetic study was carried out at 28 °C by monitoring the uptake of dyes as a function of time.

Fig. 10 represents the kinetic adsorption plot for the BR29 and BY11 dyes. Rapid uptake of dyes in initial 150 min indicated good affinity of PAA-g-Teflon adsorbent for basic dye molecules. Later the adsorption slowed down; suggesting a gradual equilibrium and finally, the saturation was reached. BY11 showed higher and faster uptake than BR29.

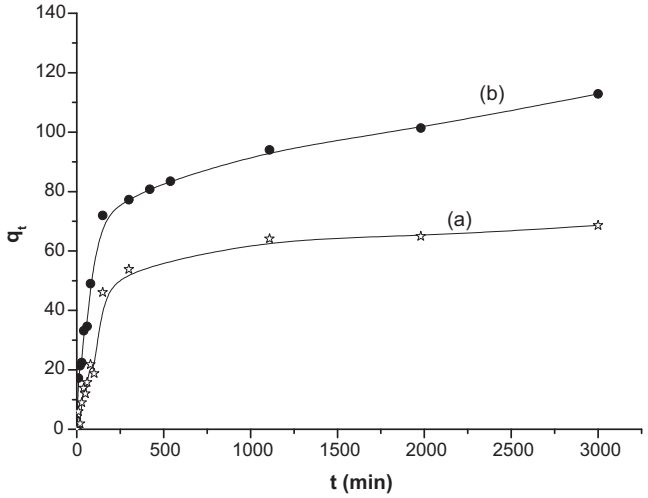

Fig. 10. Adsorption kinetics of dyes on PAA-g-Teflon (G.Y. ~30%) at 28 °C (a) BR29 (b) BY11.

3.7.1. Pseudo-first order kinetic model

The differential form of pseudo-first order equation is given as

$$\frac{d_{qt}}{dt} = k_1(q_e - q_t) \quad (16)$$

Which on integrating for the boundary conditions $q_t = 0$ at $t = 0$ to $q_t = q_t$ at $t = t$, gives Pseudo-first order linear expression, also known as Lagergren equation [17,29,30] expressed as Eq. (17)

$$\ln(q_e - q_t) = \ln(q_e) - k_1 t \quad (17)$$

where q_e (mg/g) and q_t (mg/g) are the amount adsorbed per unit mass of the adsorbent at equilibrium and at time "t" respectively, and k_1 (min^{-1}) is the pseudo-first order rate constant. The slope and intercept of the linear plot of $\ln(q_e - q_t)$ *vs* t were used to estimate the pseudo-first order rate constant k_1 (min^{-1}) and equilibrium adsorption amount $q_{e,cal}$ (mg/g), respectively. Fig. 11 and its inset shows the Lagergren plots for the adsorption of basic dyes on PAA-g-Teflon at different time scales. It is clear from the figure that adsorption follows Lagergren model only at lower time scale. In fact it has been reported that Lagergren model is applicable for initial stage of the adsorption process [31]. The pseudo-first order

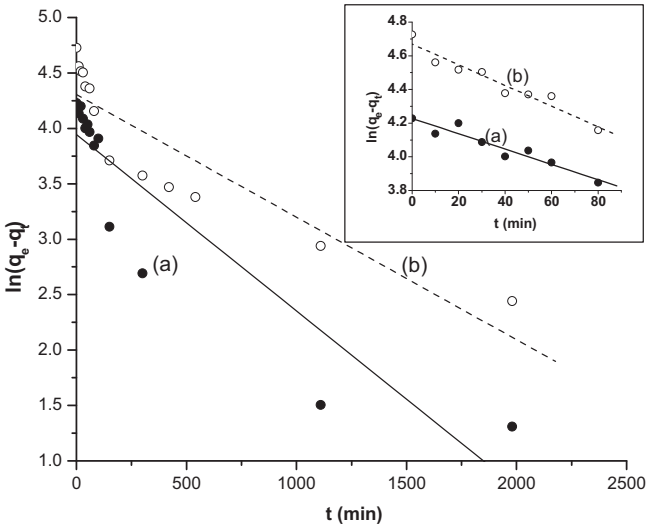

Fig. 11. Lagergren (Pseudo-first order) plots for the adsorption of dyes on PAA-g-Teflon at 28 °C (G.Y. ~30%, dye concentration = 400 ppm, pH ~4.7, 28 °C). Inset: Adsorption at lower time scale.

Table 4
Adsorption parameters for adsorption of dyes on PAA-g-Teflon adsorbent, (G.Y. = 30%, initial concentration of dyes = 400 ppm, pH 4.7).

Pseudo-first order adsorption parameters							
Dye	$q_{e,exp}$ (mg/g)	Full contact time			Initial time (upto ~80 min)		
		$q_{e,cal}$ (mg/g)	k_1 (min^{-1})	r^2	$q_{e,cal}$ (mg/g)	k_1 (min^{-1})	r^2
BR29	68.6	51.67	1.59×10^{-3}	0.8394	68.6	4.55×10^{-3}	0.9135
BY11	112.9	74.05	1.11×10^{-3}	0.8164	106.6	6.17×10^{-3}	0.9343

Pseudo-first order adsorption parameters						
Dye	$q_{e,exp}$ (mg/g)	$q_{e,cal}$ (mg/g)	k_2 (g/mg min)	h (mg/g min)	$t_{1/2}$ (min)	r^2
BR29	68.6	72.3	7.18×10^{-5}	0.38	192.4	0.9916
BY11	112.9	113.1	6.98×10^{-5}	0.89	126.6	0.9950

kinetic parameters obtained are given in Table 4. From the initial adsorption kinetic data, the pseudo-first order rate constants were found to be 4.55×10^{-3} and 6.17×10^{-3} for BR29 and BY11, respectively, which are comparable with the literature values for other dye-adsorbent systems [32].

3.7.2. Pseudo-second order kinetic model

The differential expression of the pseudo-second-order model is given as Eq. (18) [30]

$$\frac{d_{qt}}{dt} = k_2(q_e - q_t)^2 \tag{18}$$

After integrating of Eq. (18) and rearranging it gives rise to a linear expression of the pseudo-second-order model given as Eq. (19), which is mostly used for solid–liquid adsorption systems [30].

$$\frac{t}{q_t} = \frac{1}{k_2 \times q_e^2} + \frac{t}{q_e} \tag{19}$$

where k_2 is the pseudo-second-order adsorption rate constant (g/mg min); and other parameters are same as in pseudo-first order kinetic model. Predicted equilibrium adsorption amount $q_{e,cal}$ and k_2 were calculated from the slope and intercept of the linear plot. The pseudo-second-order model is generally reported to predict the behavior over the entire range of the adsorption process [30,33,34]. Pseudo-second order plot for two dyes is shown in Fig. 12. It was observed that the kinetic adsorption data for BR29 and BY11 fitted very well into pseudo-second order model unlike pseudo-first order kinetic model.

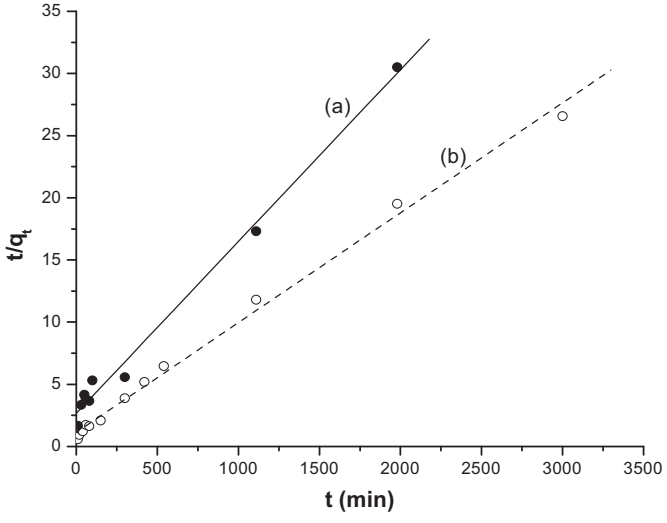

Fig. 12. Pseudo-second order plot for adsorption of dyes onto PAA-g-Teflon (G.Y. ~30%, Dye concentration 400 ppm, pH ~4.7, Temp. = 28 °C) (a) BR 29 (b) BY11.

The initial adsorption rate (h) and half-adsorption time ($t_{1/2}$) can be estimated from relations (20) and (21), respectively [27].

$$h = k_2 \times q_e^2 \tag{20}$$

$$t_{1/2} = \frac{1}{kq_e} \tag{21}$$

The Pseudo-second order kinetic parameters are given in Table 4. It can be seen that for pseudo-second-order adsorption kinetic model, the correlation coefficient values are higher (>0.99) than for pseudo-first-order kinetic model. Moreover, the calculated equilibrium adsorption capacity values ($q_{e,cal}$) were also in good agreement with experimental equilibrium adsorption capacity values ($q_{e,exp}$). These observations suggest that the adsorption of BR29 and BY11 on PAA-g-Teflon adsorbents can be approximated more appropriately by the pseudo-second-order kinetic model, over the entire range of adsorption. BY11 showed higher initial adsorption rate (h) value with lower half-adsorption time ($t_{1/2}$) as compared to that of BR29, which indicated the greater affinity of BY11 for PAA-g-Teflon adsorbent.

3.7.3. Intra-particle diffusion model

Pseudo-first order or pseudo-second order model are used to determine type and extent of adsorption. To determine the diffusion mechanism during adsorption several diffusion models have been proposed [32,34,35]. Intra-particle diffusion equation (Eq. (22)) was used to study diffusion mechanism and to determine intra-particle diffusion rate constant (k_i) (from the slope of linear plot of q_t *vs* $t^{1/2}$) of dyes on to PAA-g-Teflon adsorbent.

$$q_t = k_i \times t^{1/2} \tag{22}$$

It has been documented that if the line passes through the origin then intra-particle diffusion is the only rate determining step; otherwise, some other mechanisms along with the intra-particle diffusion are also involved which is reflected in multi-linearity of the q_t *vs* $t^{1/2}$ plot [35].

The intra-particle diffusion plot (Fig. 13) for both the basic dyes showed multi-linearity represented by two different stages, an instantaneous extremely fast uptake followed by a slow uptake suggesting involvement of two different adsorption processes. The first, fast stage represents the mass transfer of dyes through boundary layers of liquid and adsorption of dyes on the available sites on the external surface of the adsorbent. After this stage, the dye molecule enters the porous structures of the adsorbent and eventually gets adsorbed on the active sites at internal surface of the adsorbent. The transportation of dye molecule from external surface to bulk of the adsorbent sees increasing diffusion resistance, which is reflected as slower second stage adsorption. The slope of the lines in each stages is termed as the rate parameter $k_{i,n}$ (n = stage number). Rate parameters of the different stages listed in Table 5 show that the rate constant for the first adsorption stage ($k_{i,1}$) is higher than that for the second adsorption stage ($k_{i,2}$) for both

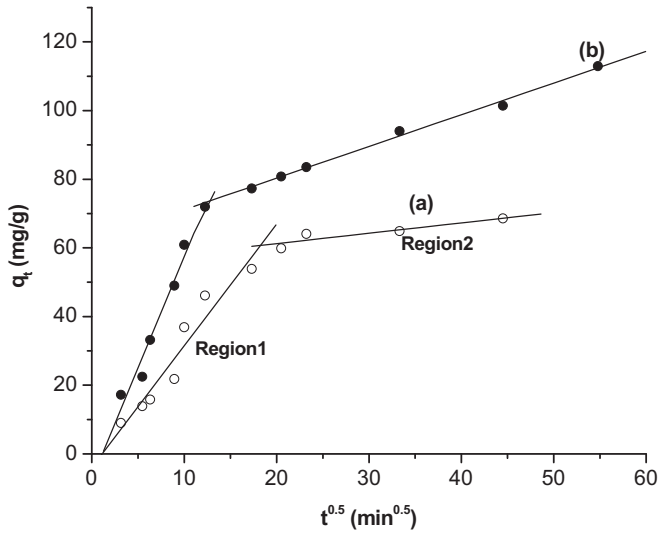

Fig. 13. The intra-particle diffusion plots for adsorption of basic dyes on PAA-g-Teflon (G.Y. ~30%, Dye concentration 400 ppm, pH ~4.7, 28 °C) (a) BR29 (b) BY11.

Table 5
The rate parameters for multi linear intra-particle diffusion profiles.

Dye	Region (1)		Region (2)	
	$k_{i,1}$ (mg/g $min^{1/2}$)	r^2	$k_{i,2}$ (mg/g $min^{1/2}$)	r^2
BR29	6.49	0.9735	0.92	0.9948
BY11	3.54	0.9263	0.30	0.8458

the dyes. Moreover, none of the linear profiles passes through origin, further establishing that intra-particle diffusion is not the only controlling process and both surface adsorption and intra-particle diffusion contribute to the rate determining step as also reported for other adsorbents–adsorbate systems [18,36].

3.8. Desorption study

The economic feasibility of the adsorption process using an adsorbent for removal of dyes from waste-water effluent is governed by its reusability for multiple adsorption–desorption cycles. In order to examine the reusability of the radiation synthesized PAA-g-Teflon adsorbent, desorption of dyes from PAA-g-Teflon adsorbent-loaded with dyes was investigated for adsorbent regeneration purpose. It was observed that both the cationic dyes once adsorbed onto the anionic PAA-g-Teflon did not desorbed even in aqueous NaCl solution of high ionic strength. This indicated adsorption of cationic dyes did not take place only by ionic interactions but some other interactions such as, hydrophobic interactions or hydrogen bonding may also be involved in the adsorption process [27]. Therefore, in present study, 1N KSCN solution in different water–methanol mixtures were used as eluent for breaking these non-specific interactions and eluting the dyes from the adsorbent [37]. The results of desorption studies are shown in Fig. 14. As can be seen from the figure the presence of methanol in the eluting solution was essential for desorption. Desorption as high as ~95% for BR29 and ~55% for BY11 was achieved in eluting mixture containing water–methanol mixture containing 60% methanol.

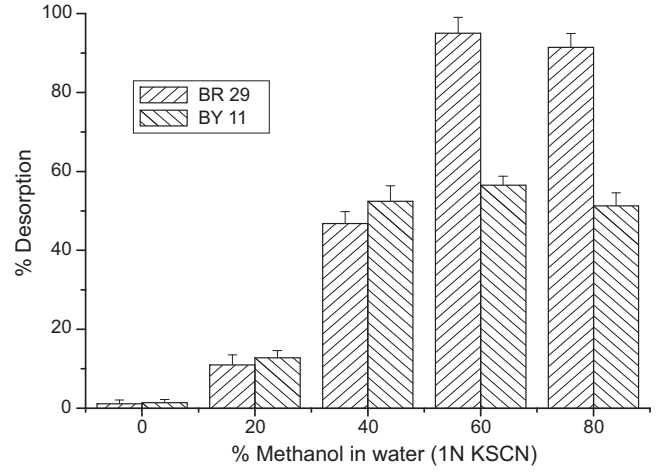

Fig. 14. Desorption of adsorbed dyes from PAA-g-Teflon in varying composition of eluent solution.

4. Conclusion

Teflon waste was successfully converted into an anionic adsorbent using radiation induced grafting. Grafting of acrylic acid on Teflon scrap to desired extent can be carried out under optimized experimental conditions. The adsorption of the basic dyes follows different adsorption isotherm models depending on structure and size of the dye molecule, and the adsorption capacity increases with temperature. Pseudo-second order kinetic model better explains the kinetics of adsorption of basic dyes. The basic dyes adsorbed on PAA-g-Teflon adsorbent can be desorbed to a great extent using eluent of suitable composition. Radiation functionalized PAA-g-Teflon adsorbent offers an attractive alternative for treatment of effluent containing dyes, which does not cause any secondary pollution.

References

[1] H. Zollinger, Color Chemistry-Synthesis Properties and Application of Organic Dyes and Pigments, VCH Publishers, New York, 1987.
[2] R. Marc, Asian textile dye makers are a growing power in changing market, Chem. Eng. News 73 (1996) 10–12.
[3] S.A. Figueiredo, R.A. Boaventura, J.M. Loureoro, Color removal with natural adsorbents: modeling, simulation and experimental, Sep. Purif. Technol. 20 (2000) 129–141.
[4] S. Chinwetkitvanich, M. Tuntoolvest, T. Panswad, Anaerobic decolorization of reactive dyebath effluents by a two-stage UASB system with tapioca as a co-substrate, Water Res. 34 (2000) 2223–2232.
[5] U. Mayer, Biodegradation of synthetic organic colorant, FEMS Symp. 12 (1981) 371–385.
[6] K.T. Chung, C.E. Cerniglia, Mutagenicity of azo dyes: structure-activity relationships, Mutat. Res. 277 (1992) 201–220.
[7] C.A. Fewson, Biodegradation of xenobiotic and other persistent compounds: the causes of recalcitrance, Trends Biotechnol. 6 (1988) 148–153.
[8] H.S. Rai, M.S. Bhattacharyya, J. Singh, T.K. Bansal, P. Vats, U.C. Banerjee, Crit. Rev. Environ. Sci. Technol. 35 (3) (2005) 219–238.
[9] J. Arundel (Ed.), Sewage and Industrial Effluent Treatment, second revised ed., Wiley-Blackwell, New York, 2000, Chapter 1.
[10] R.F. Brady Jr., Fluoropolymers, Chem. Br. 26 (1990) 427–430.
[11] R.J. Plunkett, The history of polytetrafluoroethylene: discovery and development, in: R.B. Seymour, G.S. Kirshenbaum (Eds.), High Performance Polymers: Their Origin and Development, Elsevier, New York, 1986, pp. 267–278.
[12] V. Kumar, Y.K. Bhardwaj, K. Tirumalesh, K.A. Dubey, C.V. Chaudhari, N.K. Goel, J. Biswal, S. Sabharwal, Electron beam grafted polymer adsorbent for removal of heavy metal ion from aqueous solution, Sep. Sci. Technol. 41 (2006) 3123–3139.
[13] N.K. Goel, M.S. Rao, V. Kumar, Y.K. Bhardwaj, C.V. Chaudhari, K.A. Dubey, S. Sabharwal, Synthesis of antibacterial cotton fabric by radiation-induced grafting of [2-(Methacryloyloxy)ethyl]trimethylammonium chloride (MAETC) onto cotton, Radiat. Phys. Chem. 78 (2009) 399–406.
[14] V. Kumar, Y.K. Bhardwaj, S.N. Jamdar, N.K. Goel, S. Sabharwal, Preparation of an anion-exchange adsorbent by the radiation-induced grafting of vinylbenzyltrimethylammonium chloride onto cotton cellulose and its application for protein adsorption, J. Appl. Polym. Sci. 102 (2006) 5512–5521.
[15] I. Langmuir, The constitution and fundamental properties of solids and liquids. Part I. solids, J. Am. Chem. Soc. 38 (1916) 2221–2295.
[16] H.M.F. Freundlich, Über die adsorption in lösungen, Z. Phys. Chem. (Leipzig) 57A (1906) 385–470.
[17] M.S. Chiou, H.Y. Li, Adsorption behavior of reactive dye in aqueous solution on chemical cross-linked chitosan beads, Chemosphere 50 (2003) 1095–1105.
[18] L. Semerjian, Equilibrium and kinetics of cadmium adsorption from aqueous solutions using untreated *Pinus halepensis* sawdust, J. Hazard. Mater. 173 (2010) 236–242.

[19] Y.S. Ho, J.C.Y. Ng, G. McKay, Kinetics of pollutant sorption by biosorbents: review, Sep. Purif. Methods 29 (2000) 189–232.
[20] C.V. Chaudhari, J. Paul, L. Panicker, K.A. Dubey, V. Kumar, N.K. Goel, Y.K. Bhardwaj, S. Sabharwal, Teflon scrap based cation exchanger by radiation grafting: process parameter standardization and characterization, Environ. Prog. Sustainable Energy (2010), doi:10.1002/e10533.
[21] D.K. Owens, R.C. Wendent, Estimation of the surface free energy of polymers, J. Appl. Polym. Sci. 13 (1969) 1741–1747.
[22] N.K. Goel, Y.K. Bhardwaj, R. Manoharan, V. Kumar, K.A. Dubey, C.V. Chaudhari, S. Sabharwal, Physicochemical and electrochemical characterization of battery separator prepared by radiation induced grafting of acrylic acid onto microporous polypropylene membranes, Express Polym. Lett. 3 (5) (2009) 268–278.
[23] A. Chapiro, Radiation Chemistry of Polymeric Systems, John Wiley & Sons, New York, 1962.
[24] O. Tunç, H. Tanaci, Z. Aksu, Potential use of cotton plant wastes for the removal of Remazol Black B reactive dye, J. Hazard. Mater. 163 (2009) 187–198.
[25] Y.C. Wong, Y.S. Szeto, W.H. Cheung, G. McKay, Equilibrium studies for acid dye adsorption onto chitosan, Langmuir 19 (2003) 7888–7894.
[26] R.E. Treyball, Mass Transfer Operations, third ed., McGraw Hill, New York, 1980.
[27] W. Zhijian, J. Hyeonwoo, L. Kangtaek, Kinetics and thermodynamics of the organic dye adsorption on the mesoporous hybrid xerogel, Chem. Eng. J. 112 (2005) 227–236.
[28] P. Kongkachuichay, A. Shitangkoon, N. Chinwongamorn, Thermodynamics of adsorption of lactic acid on silk, Dyes Pigm. 53 (2002) 179–185.
[29] S. Kapsabelis, C.A. Prestidge, Adsorption of ethyl(hydroxyethyl)cellulose onto silica particles: the role of surface chemistry and temperature, J. Colloid Interface Sci. 228 (2000) 297–305.
[30] Y.S. Ho, G. McKay, Pseudo-second order model for sorption processes, Process Biochem. 34 (1999) 451–465.
[31] G. Mckay, Y.S. Ho, The sorption of lead(II) ions on peat, Water Res. 33 (1999) 578–584.
[32] K.G. Bhattacharyya, A. Sharma, Kinetics and thermodynamics of Methylene Blue adsorption on Neem (*Azadirachta indica*) leaf powder, Dyes Pigm. 65 (2005) 51–59.
[33] C. Namasivayam, D. Kavitha, Removal of Congo red from water by adsorption onto activated carbon prepared from coir pith, an agricultural solid waste, Dyes Pigm. 54 (2002) 47–58.
[34] F.C Wu, R.L. Tseng, R.S. Juang, Kinetic modelling of liquid-phase adsorption of reactive dyes and metal ions on chitosan, Water Res. 35 (2001) 613–618.
[35] C.K. Lee, K.S. Low, L.C. Chung, Removal of some organic dyes by hexane-extracted spent bleaching earth, J. Chem. Technol. Biotechnol. 69 (1997) 93–99.
[36] V.L. Snoeyink, R.S. Summers, Adsorption of organic compounds, Water Quality and Treatment: A Handbook of Community Water Supplies, fifth ed., MaGraw-Hill Inc., New York, 1999.
[37] C.H. Liu, J.S. Wu, H.C. Chiu, S.Y. Suen, K.H. Chu, Removal of anionic reactive dyes from water using anion exchange membranes as adsorbers, Water Res. 41 (2007) 1491–1500.